2021 French-Ukrainian Workshop
Instrumentation developments for High energy physics

A portable gamma camera for the optimization of the patient dosimetry in radioiodine therapy of thyroid diseases

T. Bossis[a], M.-A. Verdier[a,c], L. Pinot[a], F. Bouvet[a], T. Beaumont[b], D. Broggio[b], A. Desbrée[b], O. Caselles[d], S. Zerdoud[d], L. Ménard[a,c]

[a] Université Paris Saclay, IJCLab CNRS-IN2P3, F-91405 Orsay, France.

[b] Laboratory of Internal Dose Assessment, IRSN, Fontenay-aux-roses, France

[c] Université de Paris, IJCLab CNRS-IN2P3, F-91405 Orsay, France.

[d] Institut Claudius Regaud, IUCTO, TOULOUSE, France

Molecular Radiotherapy

Radiopharmaceutical

Radionuclide + Molecule

Cells irradiation through β^- or α decays

Cell targeting

Most diffuse MRT procedures in Europe (42.500 treatments in 2015)

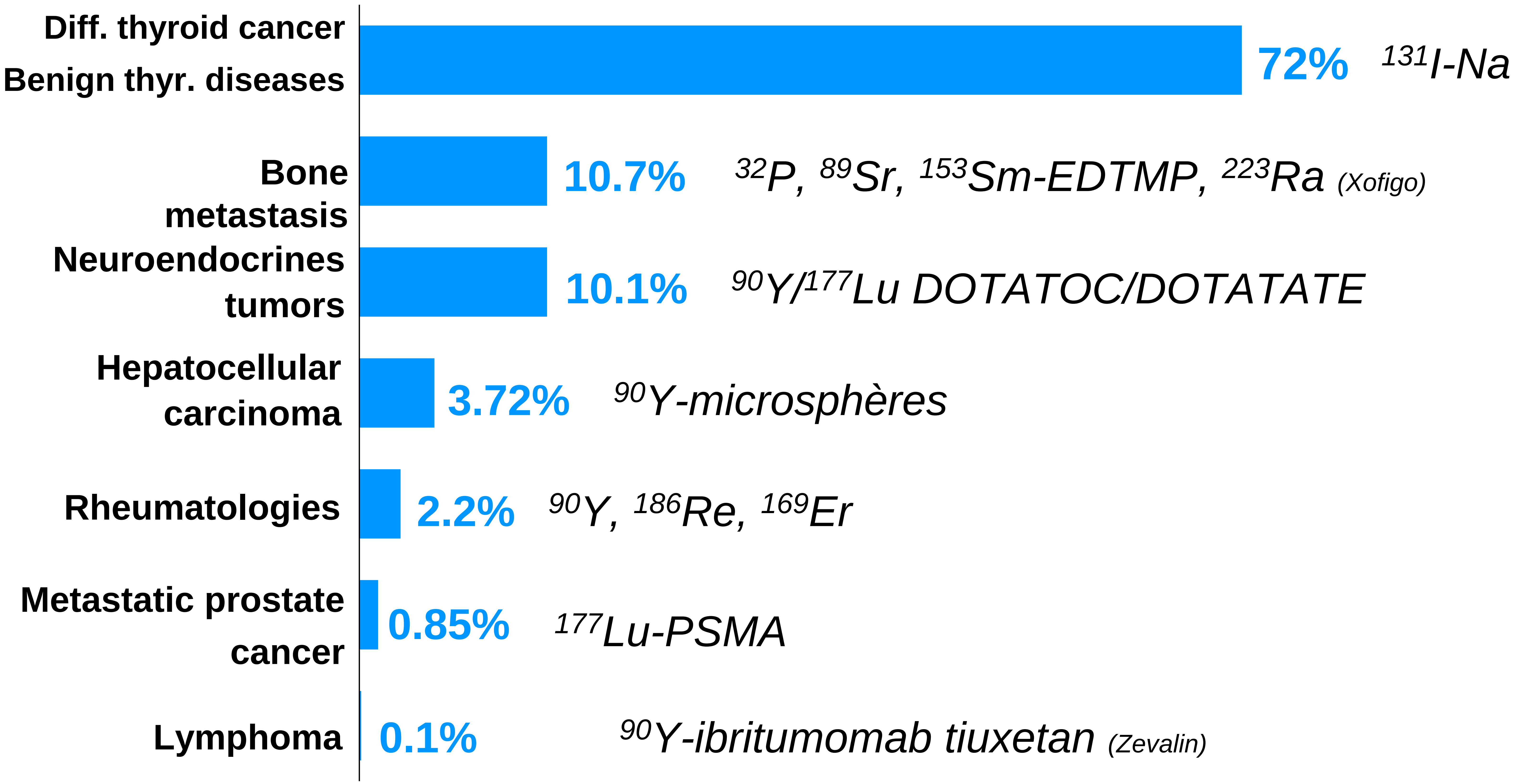

Towards more targeted therapies : new radiopharmaceuticals (peptides, antibodies) combined with novel radionuclides emitting alpha (^{211}At, ^{225}Ac, ^{149}Tb,…) or beta (^{47}Sc, ^{67}Cu, ^{177}Lu, ^{212}Pb,…) particles

Molecular Radiotherapy

Necessary to minimize the effect to healthy cells, while maximizing those of the target for which the radiological treatment is intended

- ✓ Big differences in the observed effects (response and toxicity) [1]
- ✓ Effects are dependent on the <u>Absorbed dose</u> (Gy = J/kg) delivered to the tissues [1]

Need of a <u>personalized dosimetry</u> to reach the highest reasonably achievable treatment efficiency

[1] Strigari, Lidia, et al. "The evidence base for the use of internal dosimetry in the clinical practice of molecular radiotherapy." European journal of nuclear medicine and molecular imaging 41.10 (2014): 1976-1988.

Role of dosimetry in internal radiotherapy

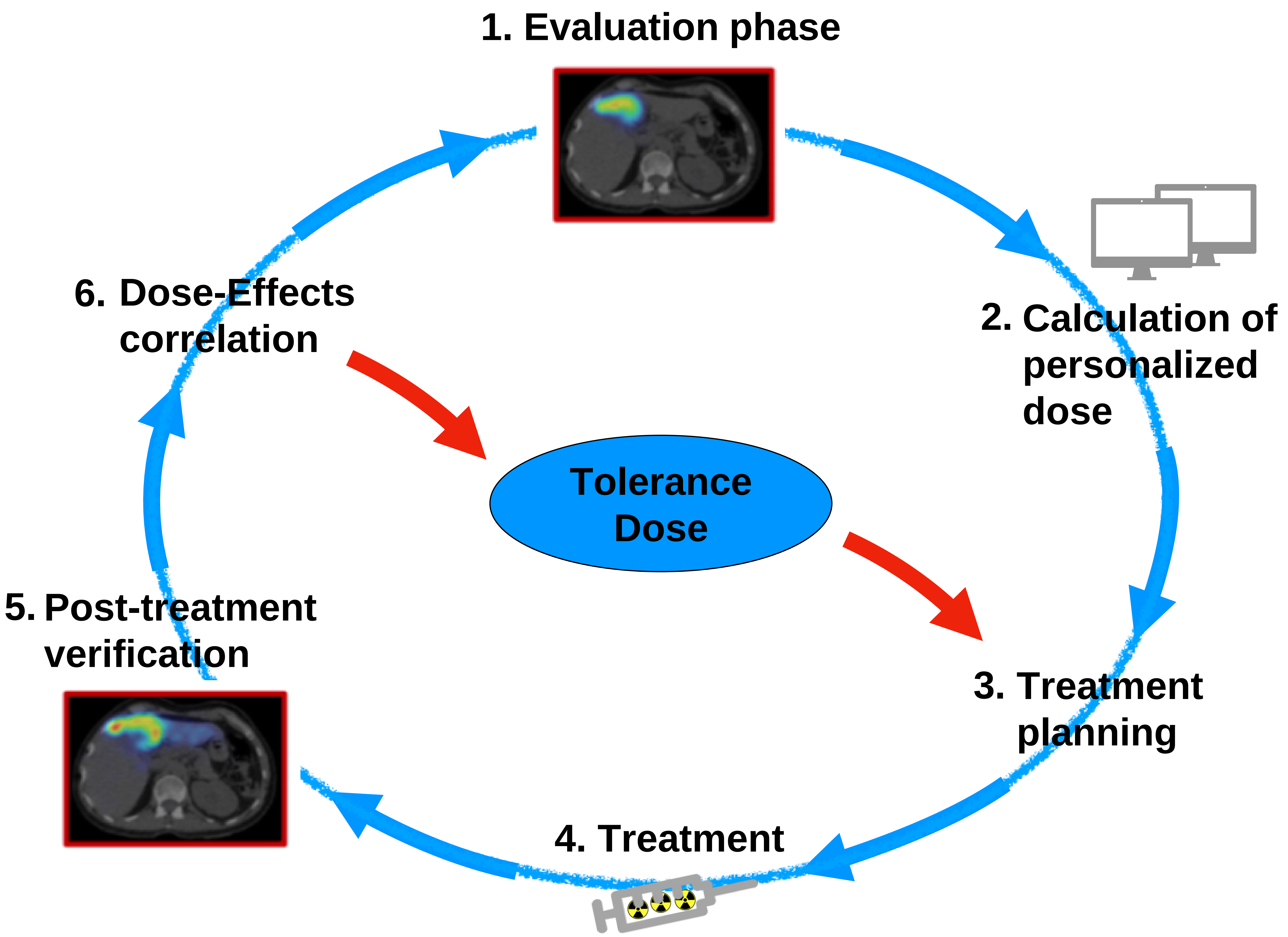

Dose-based treatment planning : determine the activity to be injected according to the desired clinical outcomes and tolerance doses of organs at risk

Post-treatment verification : control that the absorbed dose corresponds to the one estimated from the evaluation phase

Correlation between the dose released to the tumors/organs at risk and the clinical effects

Challenges and constraints of dosimetry for MRT

Why lack of dosimetry-based treatment planning and post-treatment verification nowadays?

Existing protocols considered to be well working

Dosimetric protocols are heavier and time consuming

Patient accessibility (radiation safety)

No availability of the existing cameras for treatment imaging

Lack of specified gamma cameras for quantitative imaging

Challenges and constraints of dosimetry for MRT

Improve the individual quantitative assessment of the heterogeneous distribution and biokinetics of ^{131}I before and after treatment administration for thyroid diseases

Development of a high-resolution mobile camera, 10x10cm^2 Field of View, for imaging with high energy gamma rays (>300 keV) **and high photon fluence rates** (200 kcps @ 364 keV)

Mobility to perform exams at the patient's bedside or in an isolated room for an accurate temporal sampling of the ^{131}I biokinetics

Compactness to improve image contrast (reduced camera/source distance and optimized angular view)

High spatial resolution (3 to 6 mm FWHM) to improve detectability and quantification of small activity heterogeneities (reduction of the partial volume effect)

High energy resolution (<8% FWHM @ 364 keV) to reduce scatter from high energy gamma rays

Design of the miniaturized gamma camera

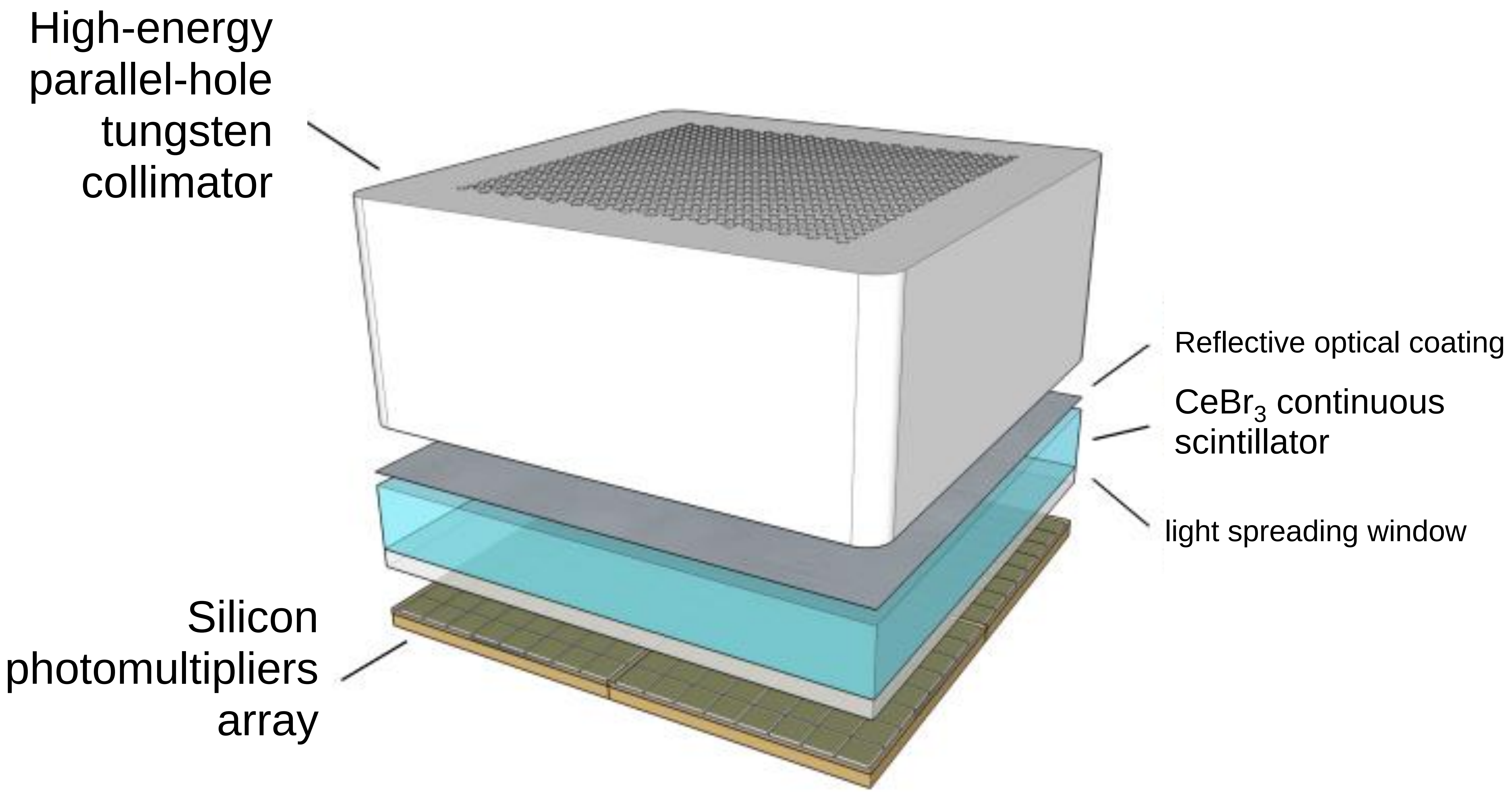

Proof of concept prototype

$5x5cm^2$ FoV proof of concept prototype

Design :

- 256 Hamamatsu S13361-6050NE-04 monolithic arrays ($3x3\ mm^2$/50µm) mounted on a single PCB (Four 8x8 arrays)
- Custom acquisition electronics made at LAL Laboratory
- 6mm thick $CeBr_3$ continuous scintillator with reflective coated edges

Intrinsic performances :

- Energy resolution @ 364 keV : 7.86% FWHM
- Spatial resolution : 0.61 mm FWHM
- Acquisition rate : ~13 kcps

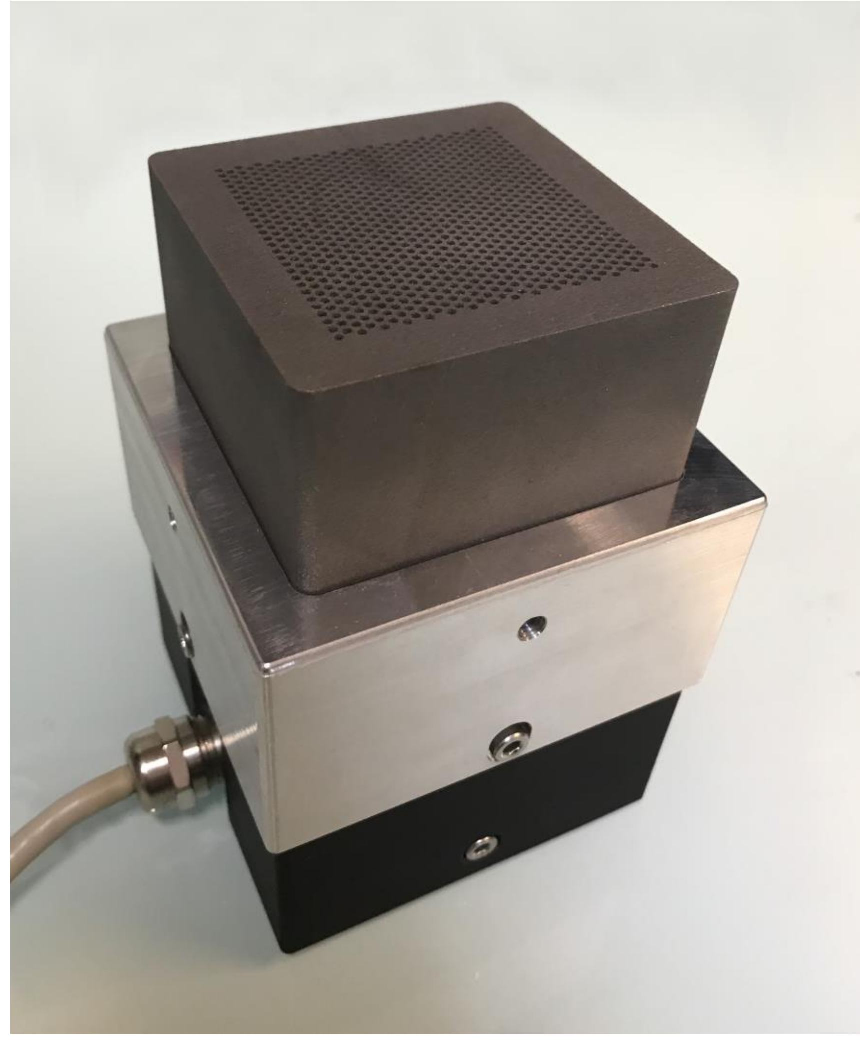

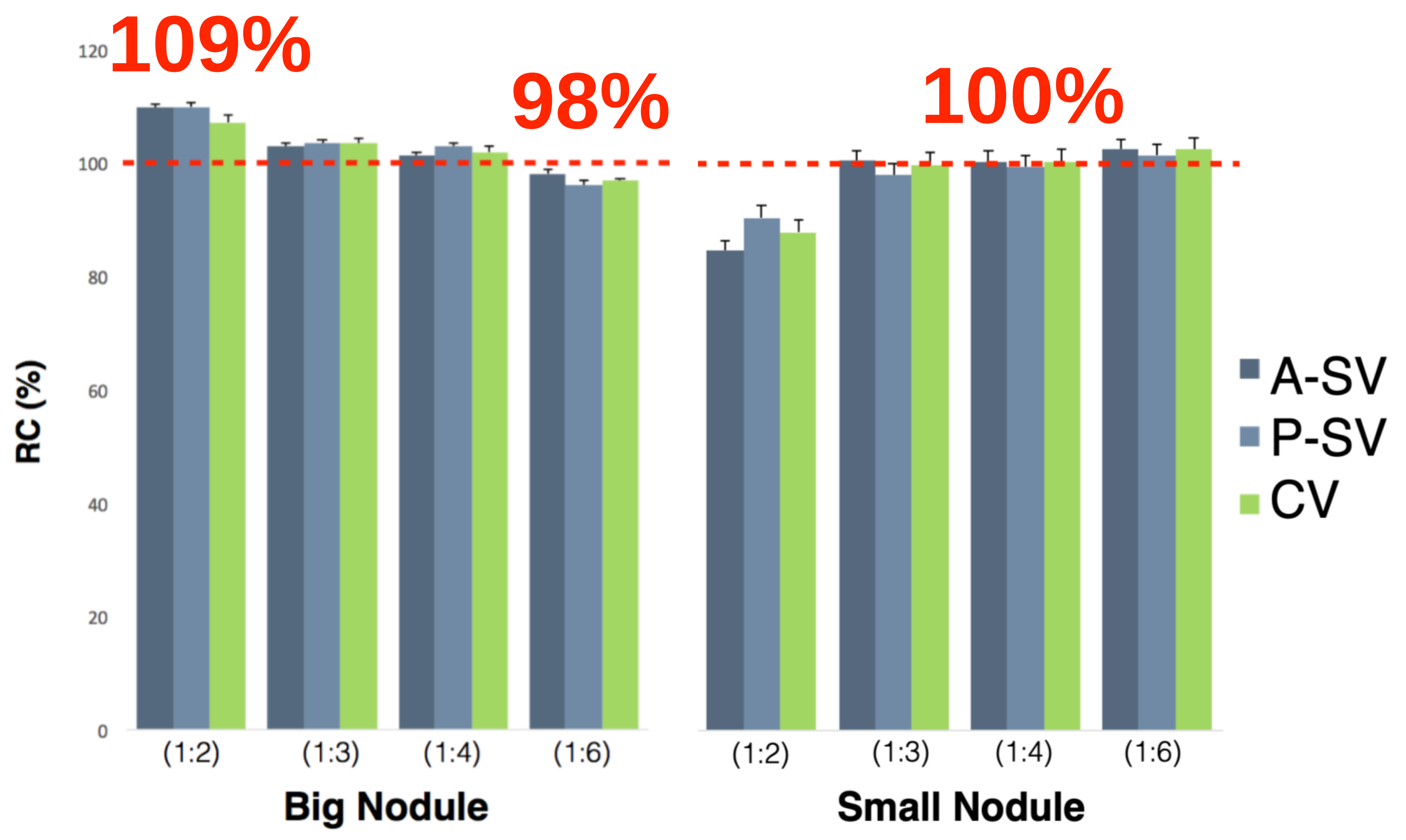

Thyroid phantoms (IRSN)

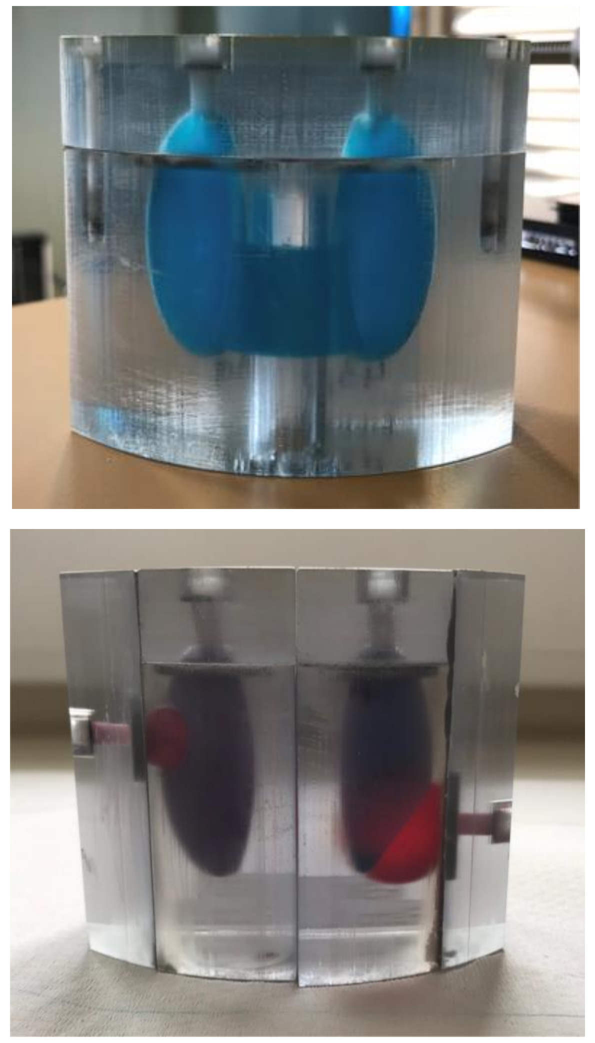

Mobile camera Anterior (A) view
SR 3.1 mm @ 5cm

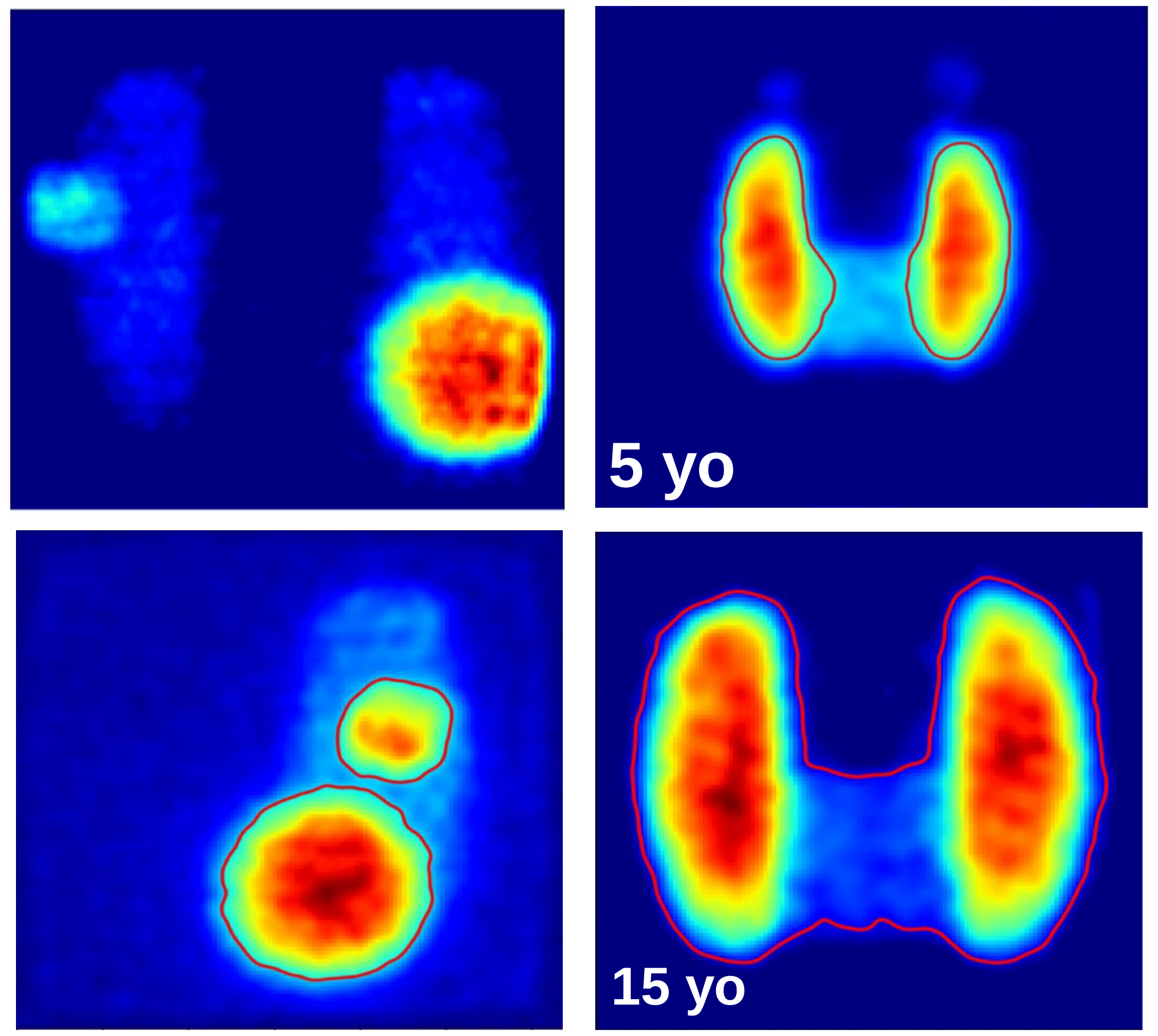

Siemens Symbia T2
SR 13.4 mm @ 10 cm

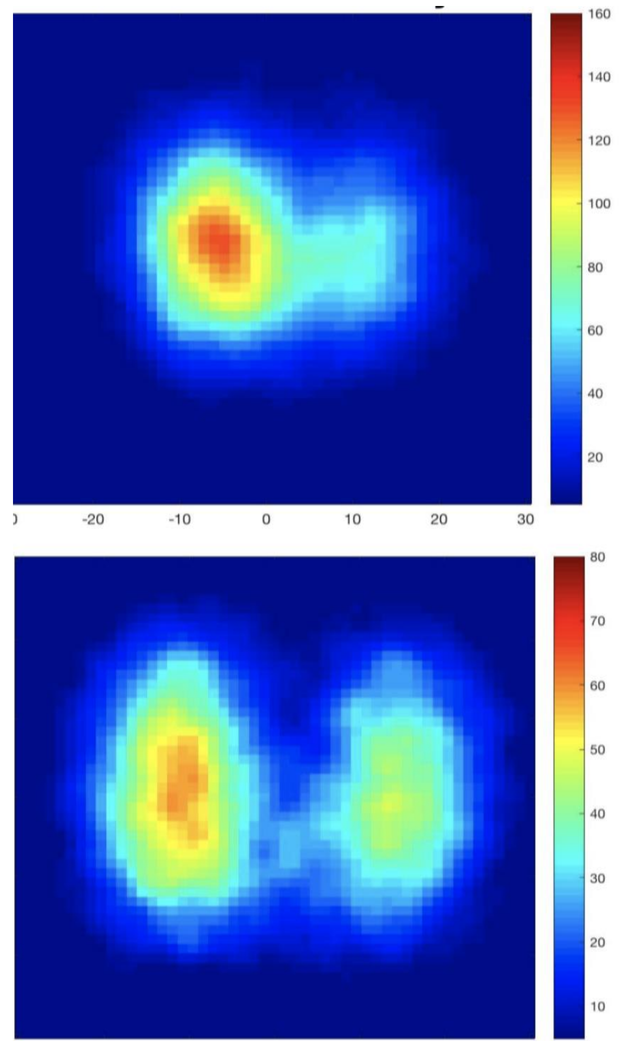

$10x10cm^2$ Field of View clinical prototype

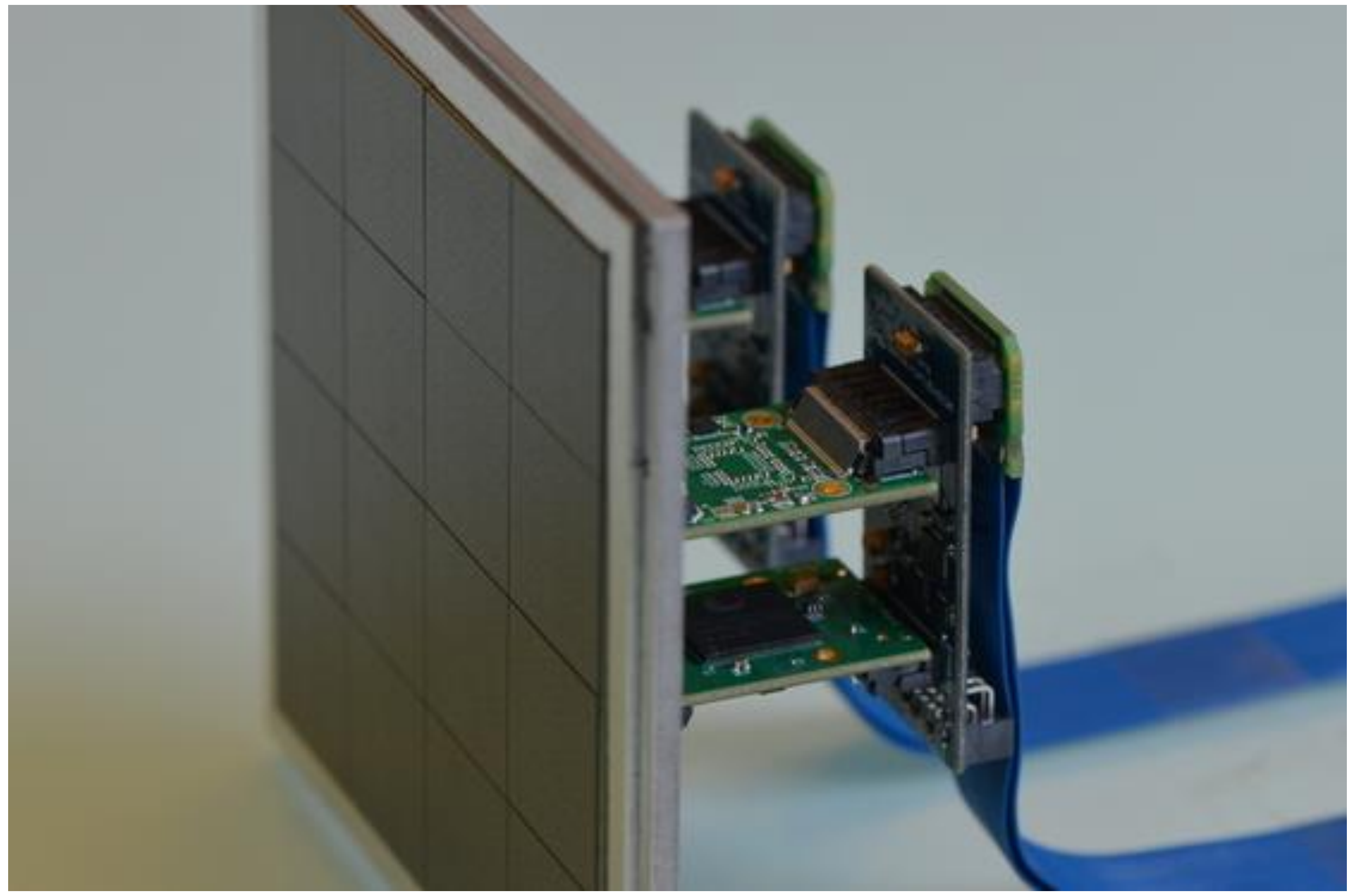

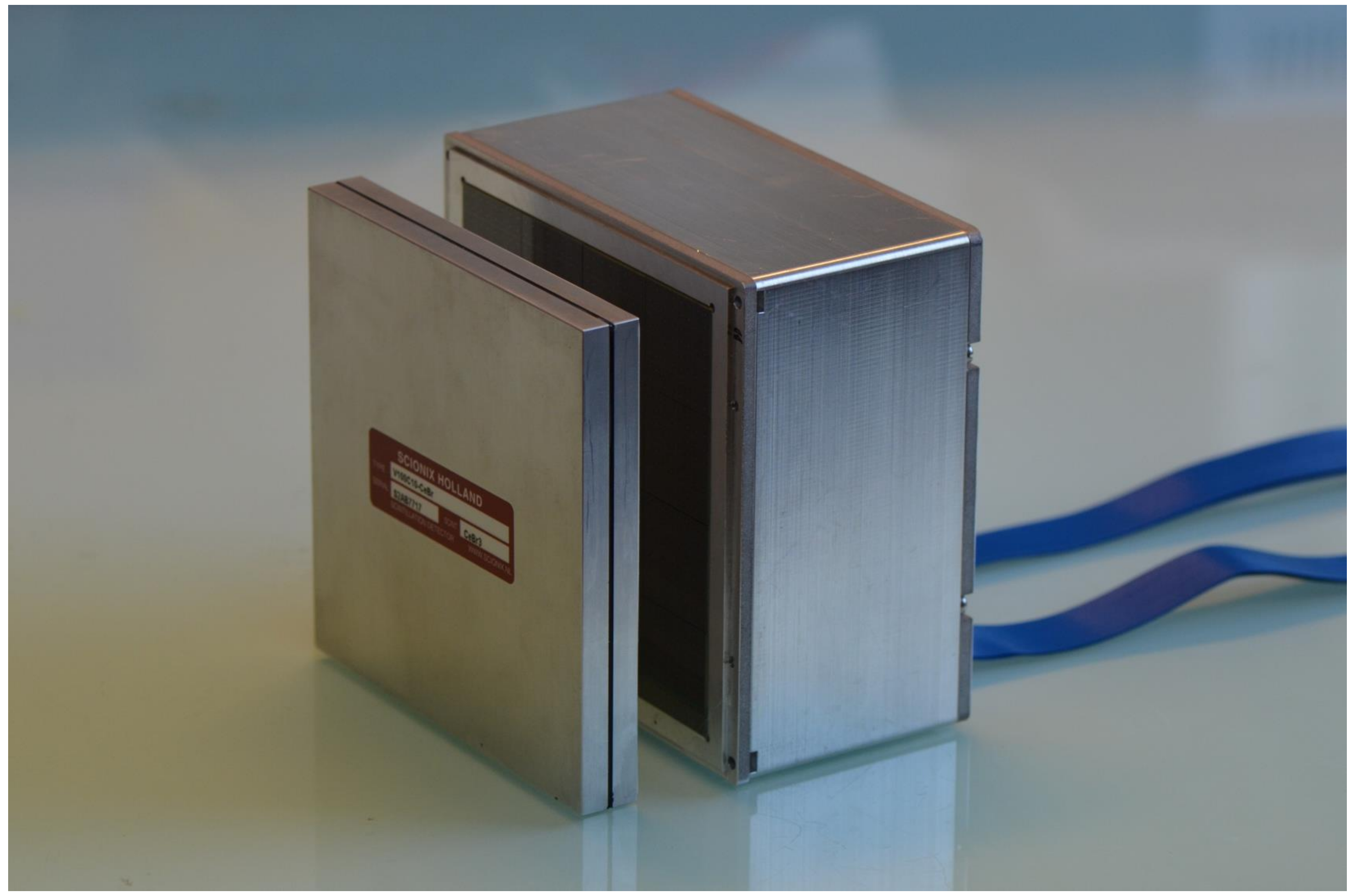

The photodetection system

- 256 Hamamatsu S13361-6050NE-04 monolithic arrays (6x6 mm^2/50µm) mounted on an interface PCB (Sixteen 4x4 arrays)
- $10x10cm^2$ and 1 cm thick $CeBr_3$ continuous scintillator with reflective coated edges
- Commercial acquisition electronics (TOFPET 2B ASICs - PETSys Electronics)
- Spatial coincidence trigger to reject dark counts
- Acquisition rate of ~50 kcps

Intrinsic performances : energy response

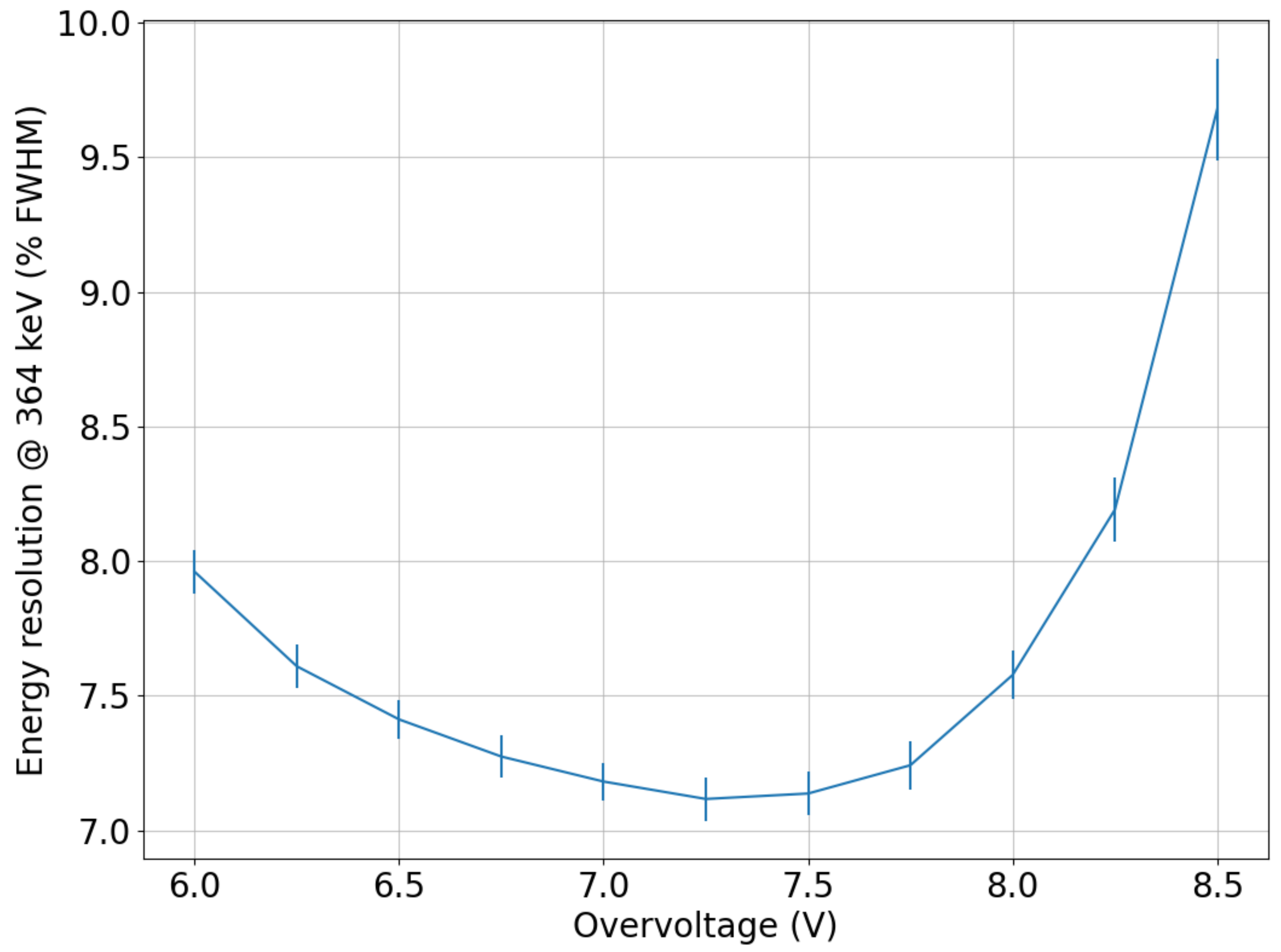

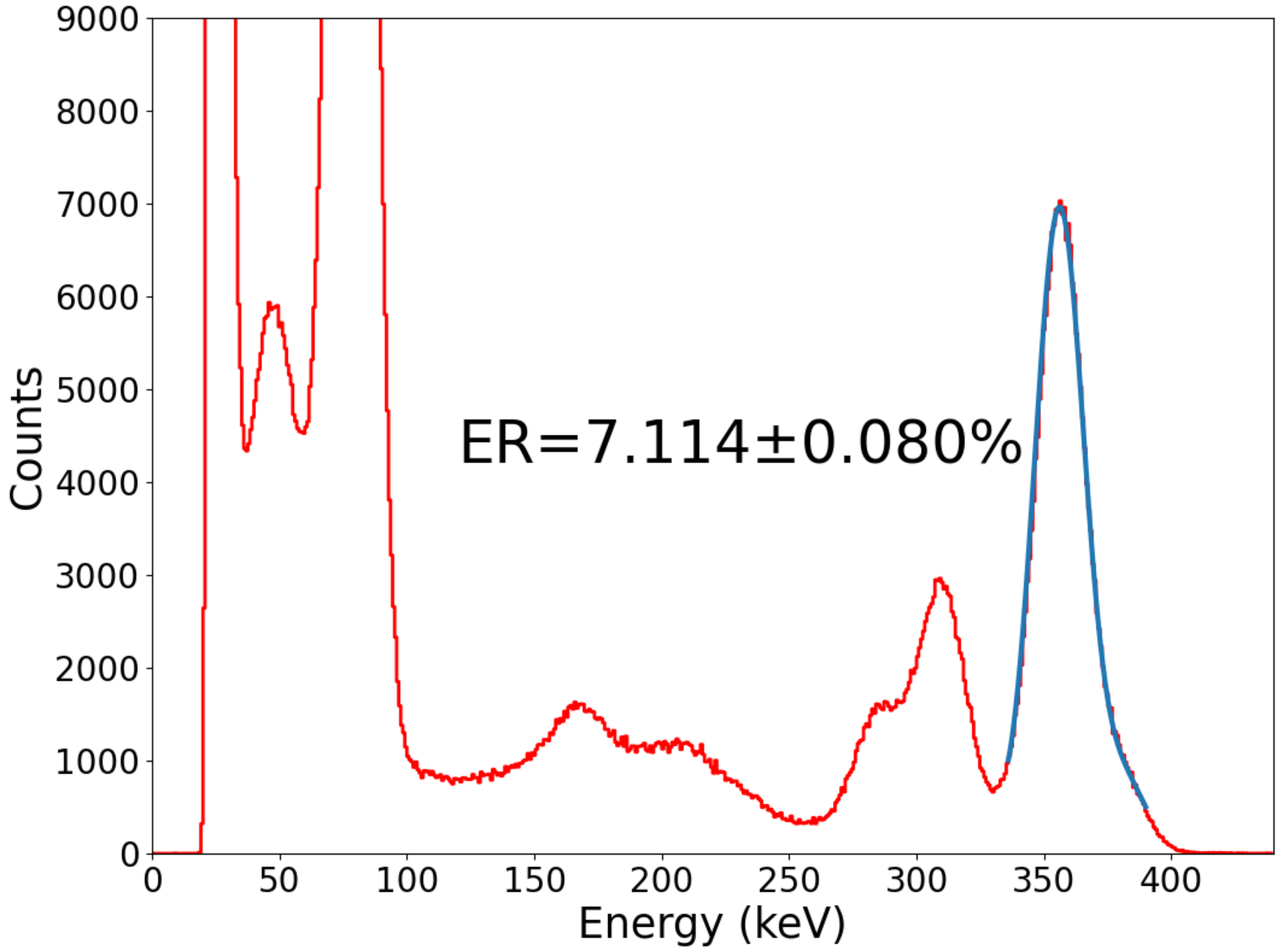

5x5cm^2 test setup design :

- 64 SiPMs of 6x6mm^2 sensitive area (four 8x8 arrays)
- 6 mm thick CeBr3 continuous scintillator
- PETSys acquisition electronics

Intrinsic performances evaluation :

- Climatic chamber at 21°C
- Collimated ^{133}Ba source (356 keV) mounted on a 3D motorized platform

Intrinsic performances : image reconstruction algorithms

2 image reconstruction algorithms

Complete scan of the FoV with a 0.5 mm collimated ^{133}Ba source (356 keV)

Fitting method (1)

Light function response measured by a reference scan providing the mean light distribution for each position (300 evts/spot)

Reconstruction of the event position by fitting the interpolated light distribution from the reference scan (mean squared error minimization)

Neural Network (2)

Training dataset (500 evts/spot)

Supervised training of a Deep Residual Convolutional neural network on the shuffled dataset

Architecture : 3 layers (64/128/256) - 3x3 kernel

Validation of generalization capability on a flood field uniformity acquisition

Intrinsic performances : spatial response

(1) (2)

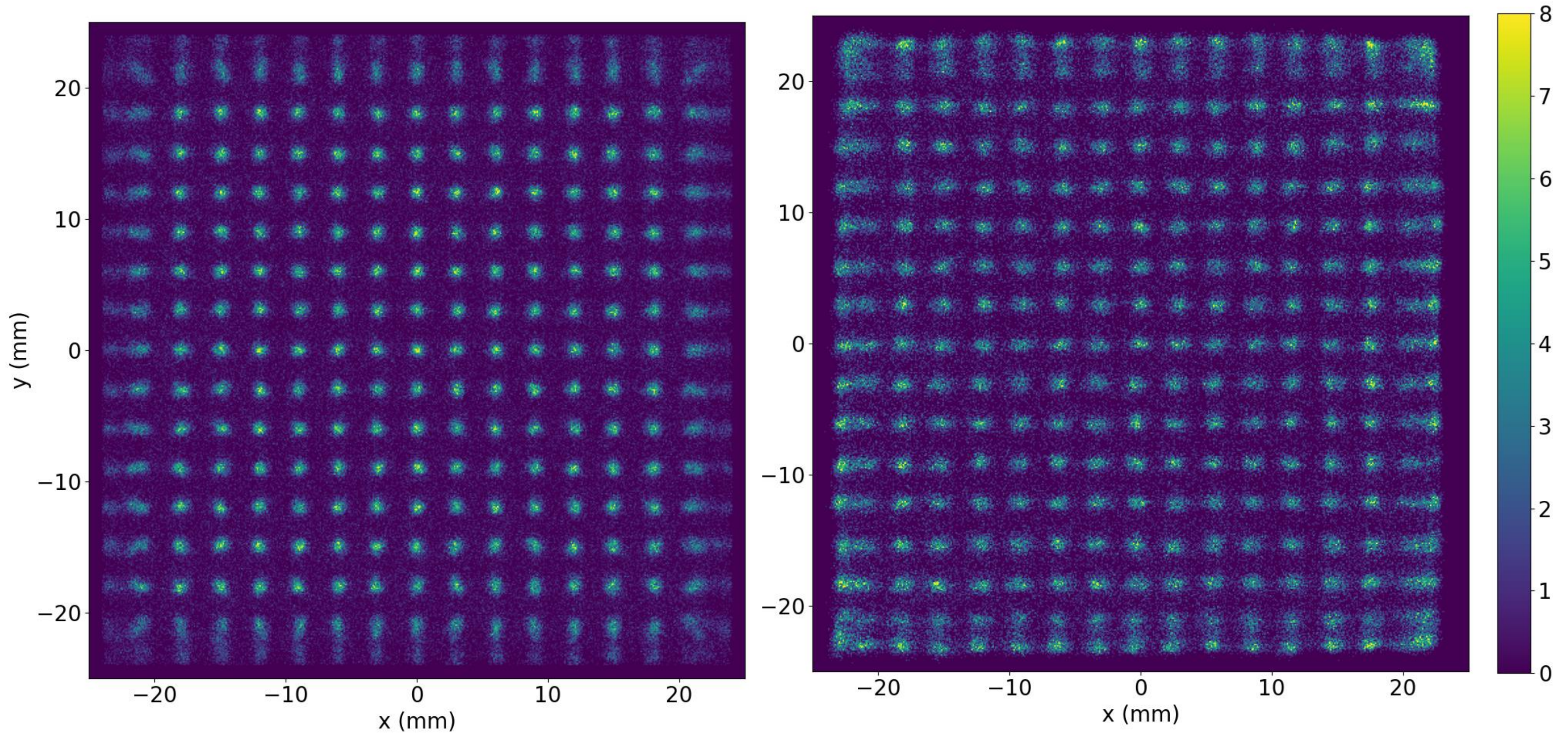

Fitting (1)

Reconstruction of a 17x17 scan (3mm step) with a reference scan of 25x25 (2mm step)

Resolution FWHM (mm) CFOV	0.73±0.06
Distortion (mm) CFOV	0.06±0.03
Maximum distortion (mm)	1.66
Integral uniformity CFOV	16.19%
Differential uniformity CFOV	11.51%

Neural Network (2)

Reconstruction of a 17x17 scan (3mm step)

Resolution FWHM (mm) CFOV	1.06±0.13
Distortion (mm) CFOV	0.67±0.21
Maximum distortion (mm)	2.99
Integral uniformity CFOV	20.96%
Differential uniformity CFOV	11.80%

Spatial Resolution Map

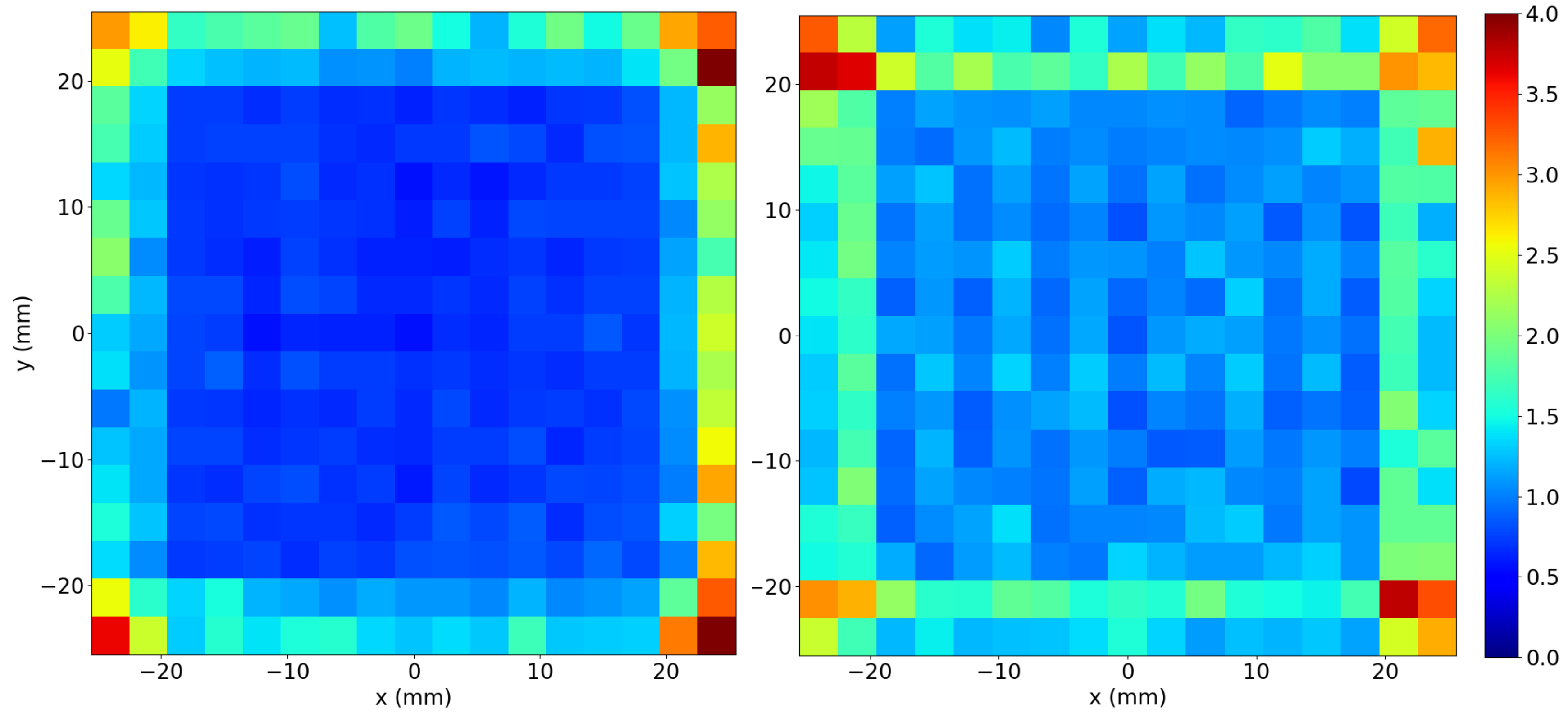

(1) (2)

Distortion Map

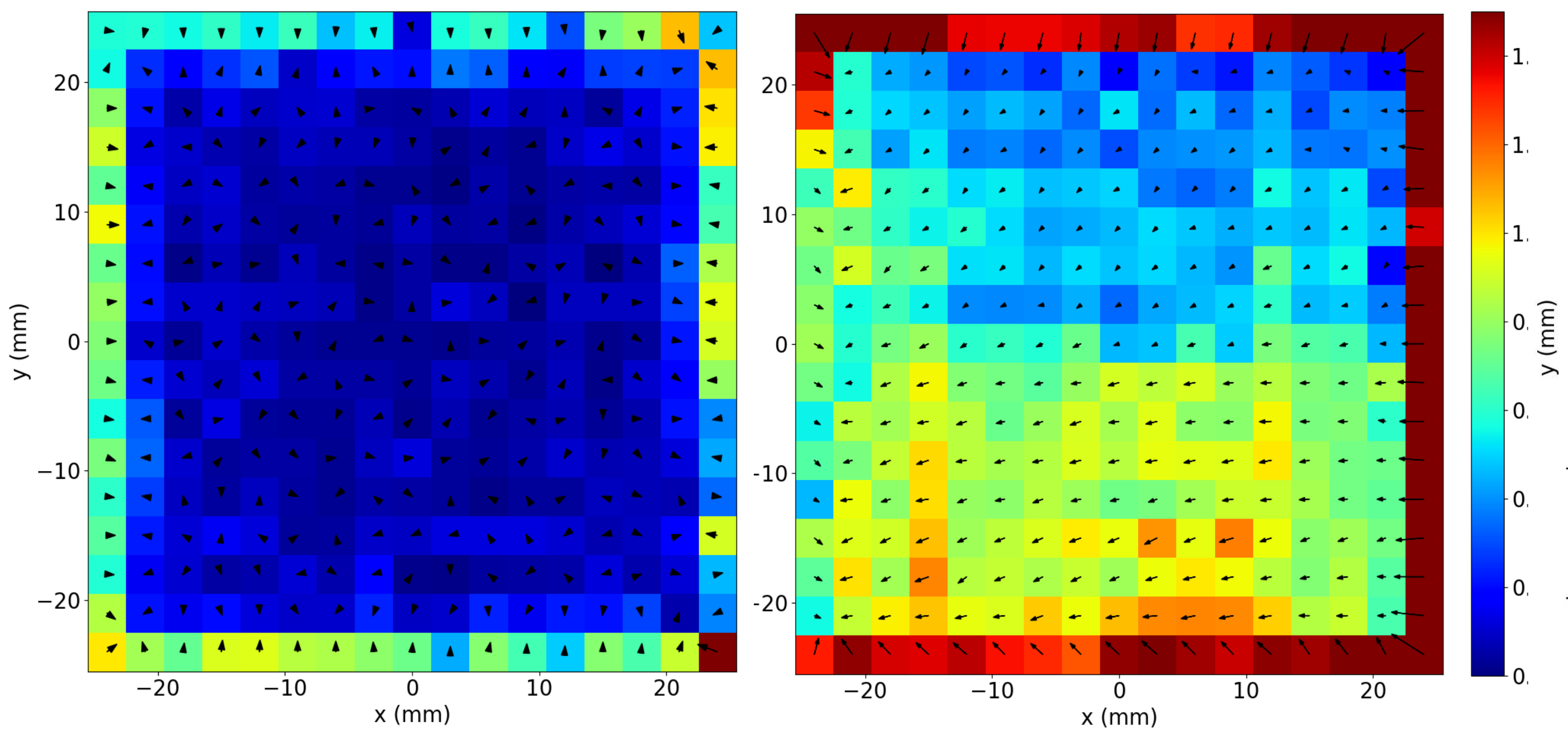

(1) (2)

Flood Field Uniformity

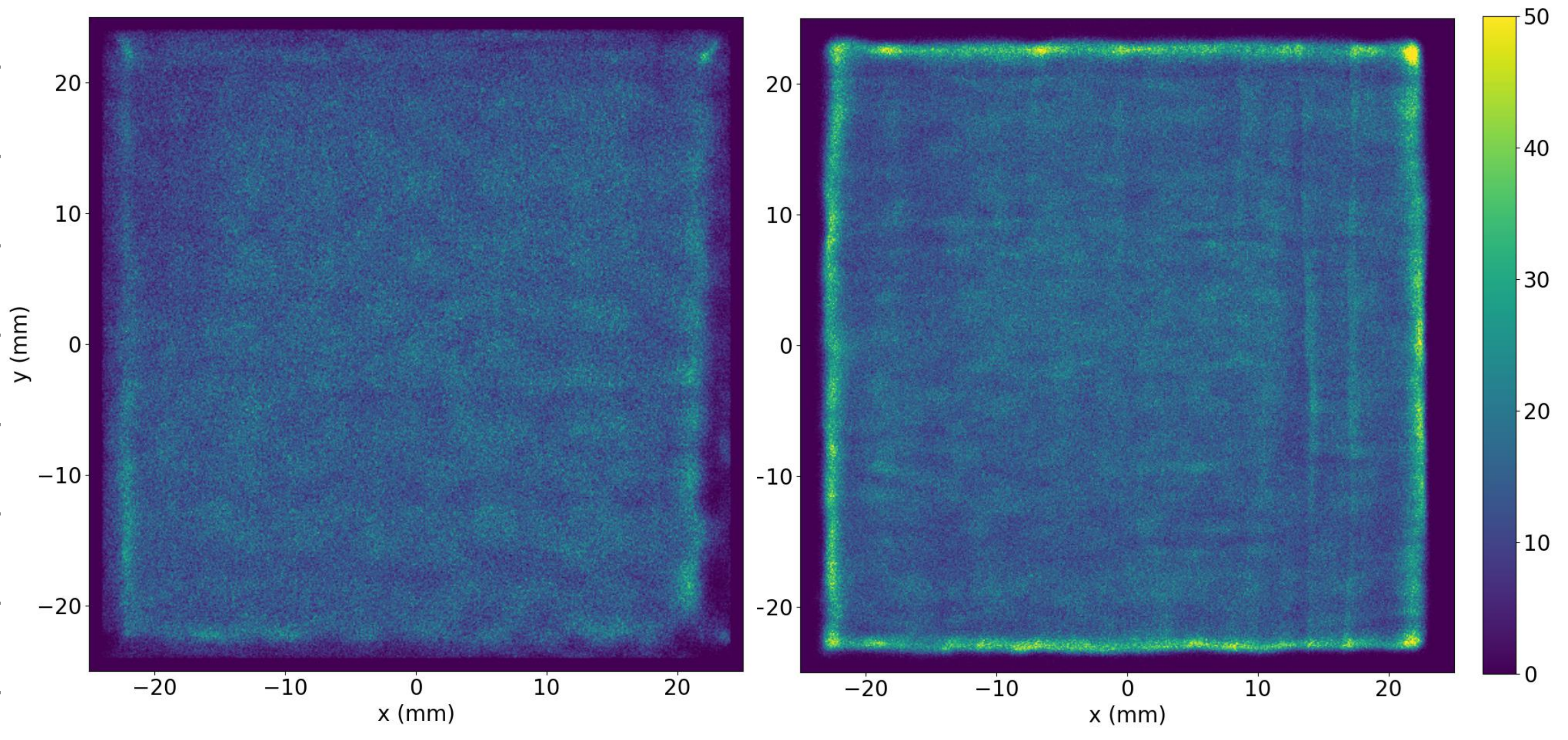

(1) (2)

The high energy parallel-hole collimator

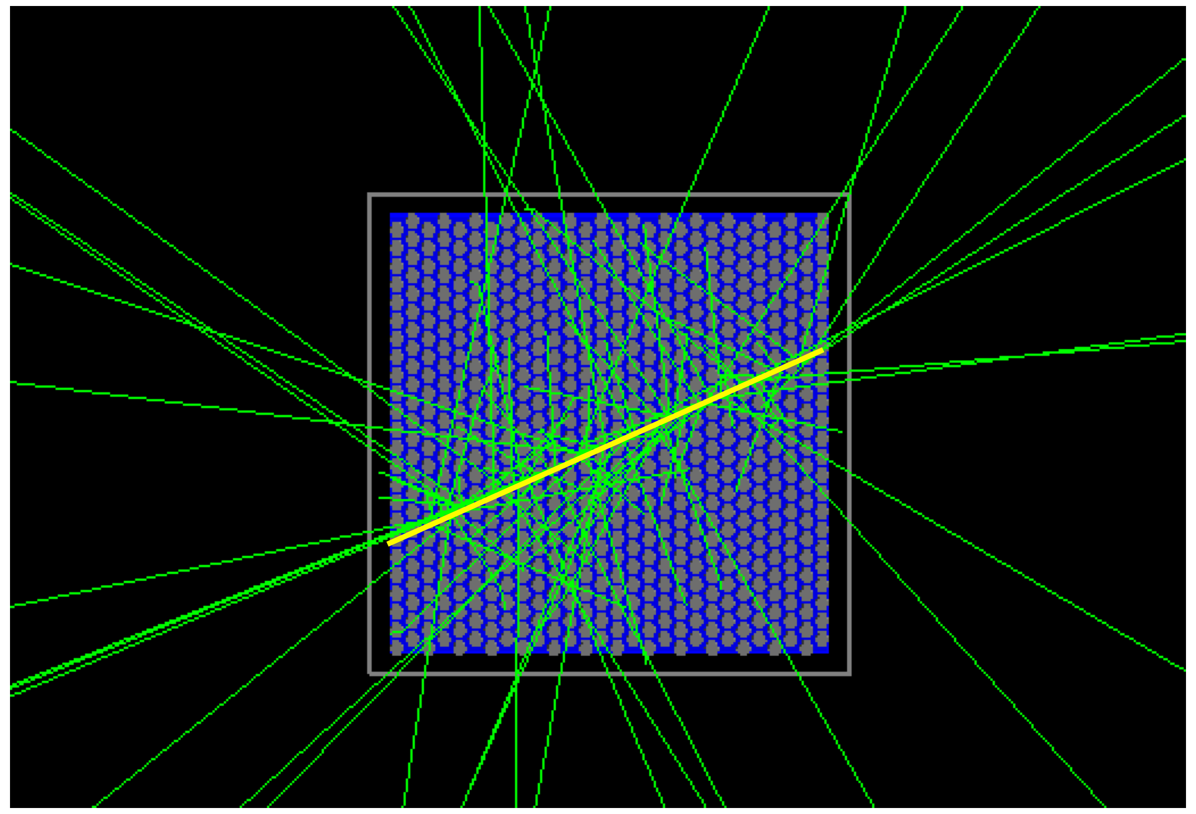

Effective septal penetration
(%Total events)

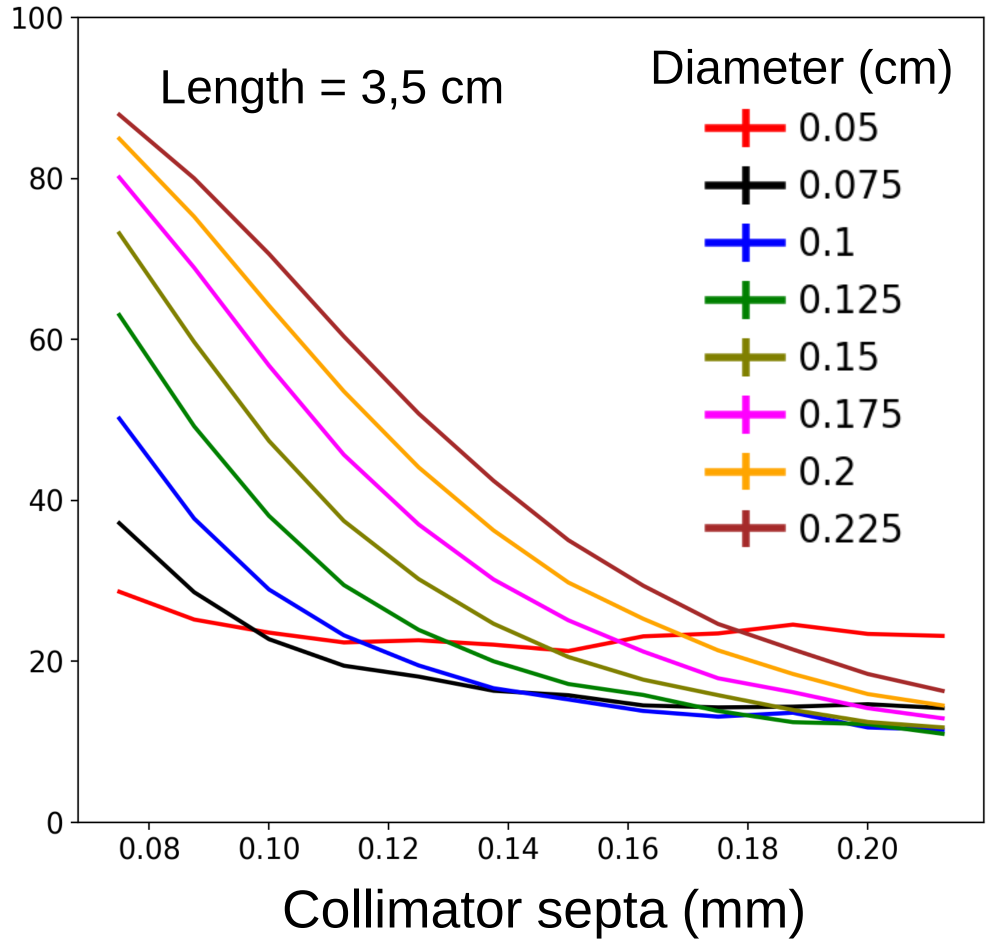

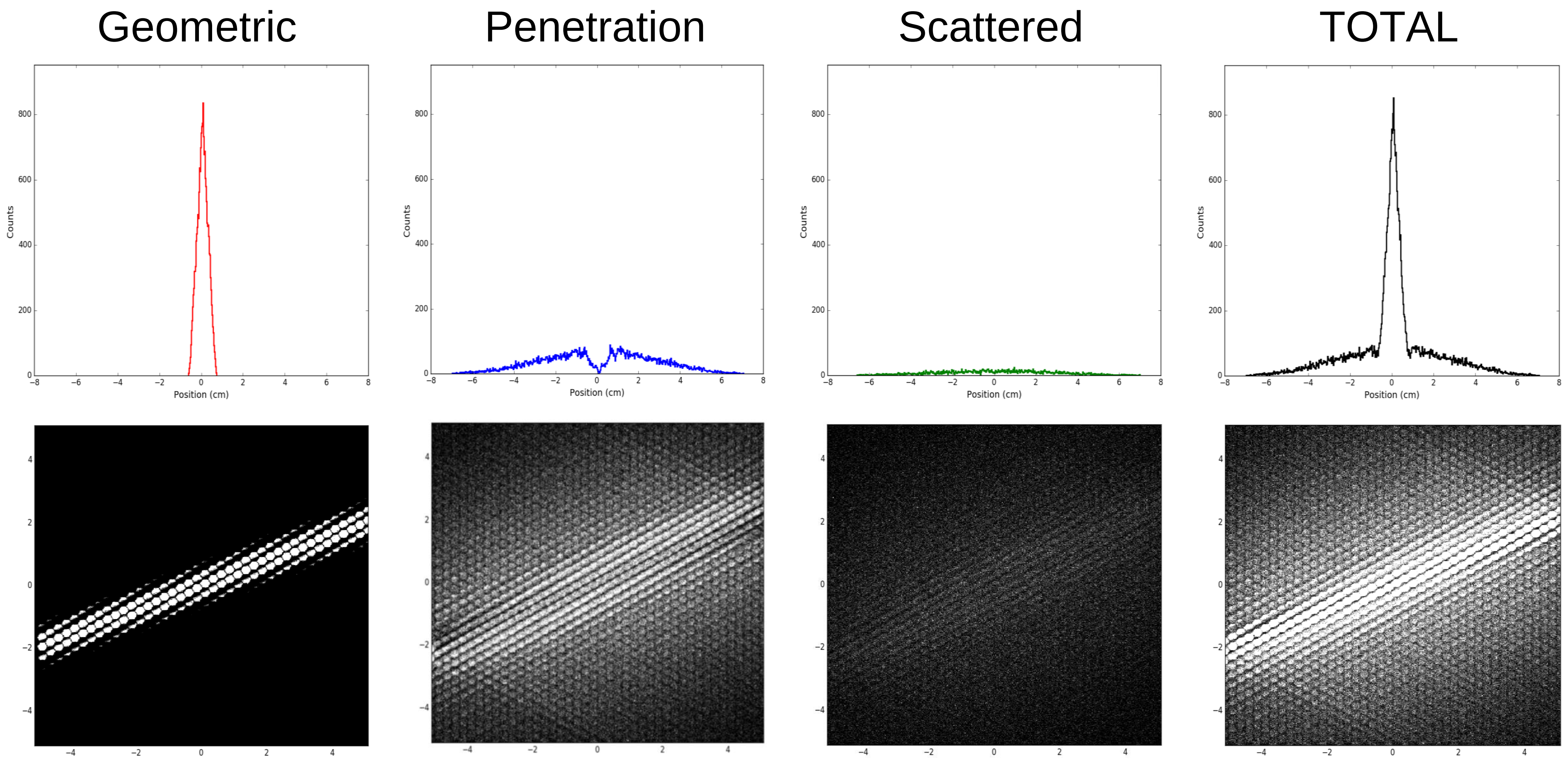

Optimization study based on Monte Carlo simulations (GATE) and analytical models

All configurations with effective septal penetration of 7.5 %

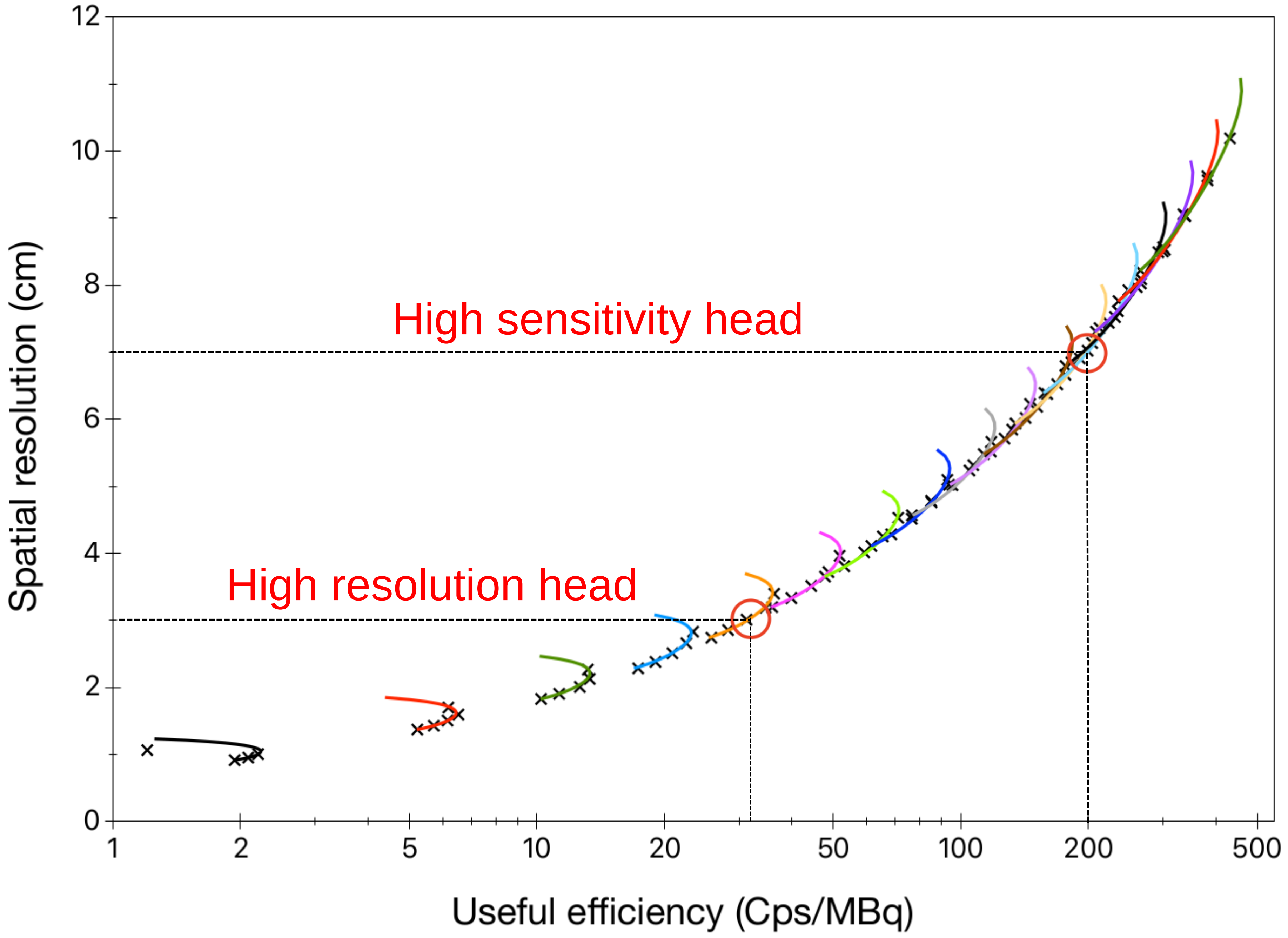

	L (cm)	*d (mm)*	*t (mm)*	*SR (mm) @ 5 cm*	*Efficiency (Cps/MBq) @ 5 cm*
Planning	5.87	1.8	0.84	3	32
Control	5.44	4.02	1.69	7	200

The high energy parallel-hole collimator

3D printing with a selective laser melting procedure

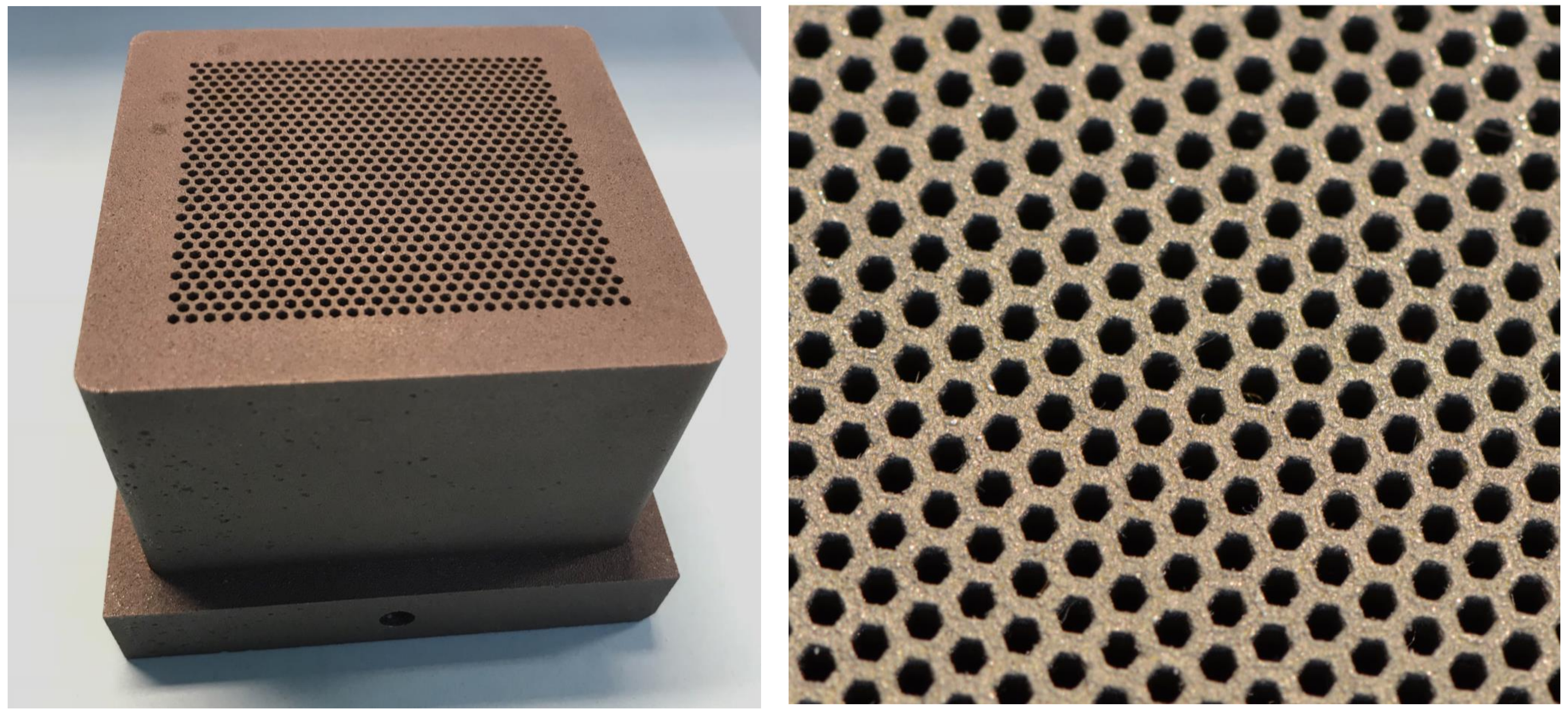

Collimator of the Proof of Concept prototype (M&I Materials)

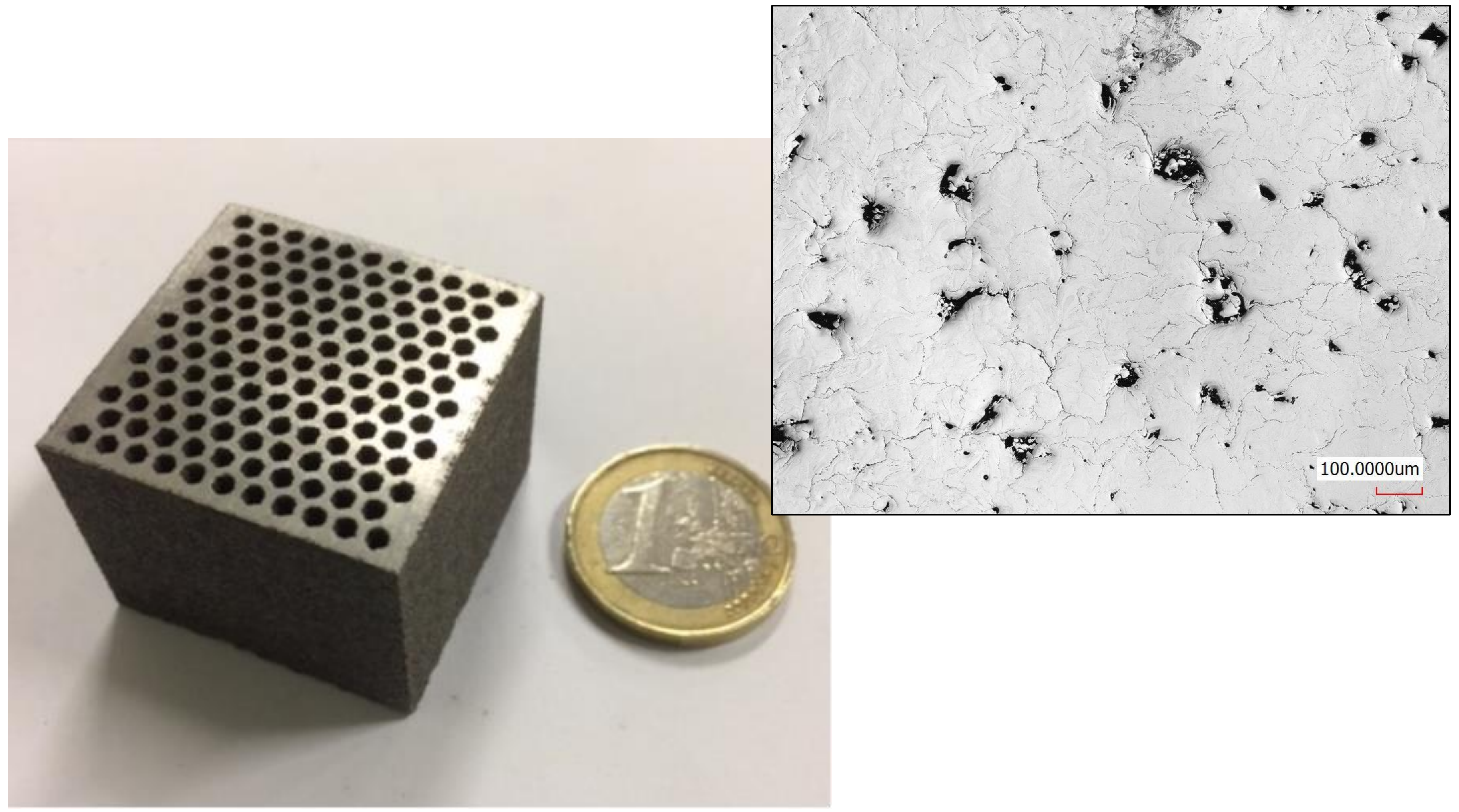

Tungsten sample for 3D printing optimization (UTBM, Belfort)

Maximal effective density 18,7 g.cm^{-3}
compared to 19,3 g.cm^{-3} for bulk tungsten (measured with Mercure intrusion porosimetry, ICB Laboratory)

Open/total porosities : 1,8/5% (1.7 to 2.5 µm)

Optimization of shielding through Monte Carlo simulation (Gate)

Sensitivity of the camera for each simulated organ + biokinetics given by the Leggett model [1]

Signal (activity coming from the thyroïd) to noise (activity coming from other organs) ratio over time

XCAT Voxelized phantom

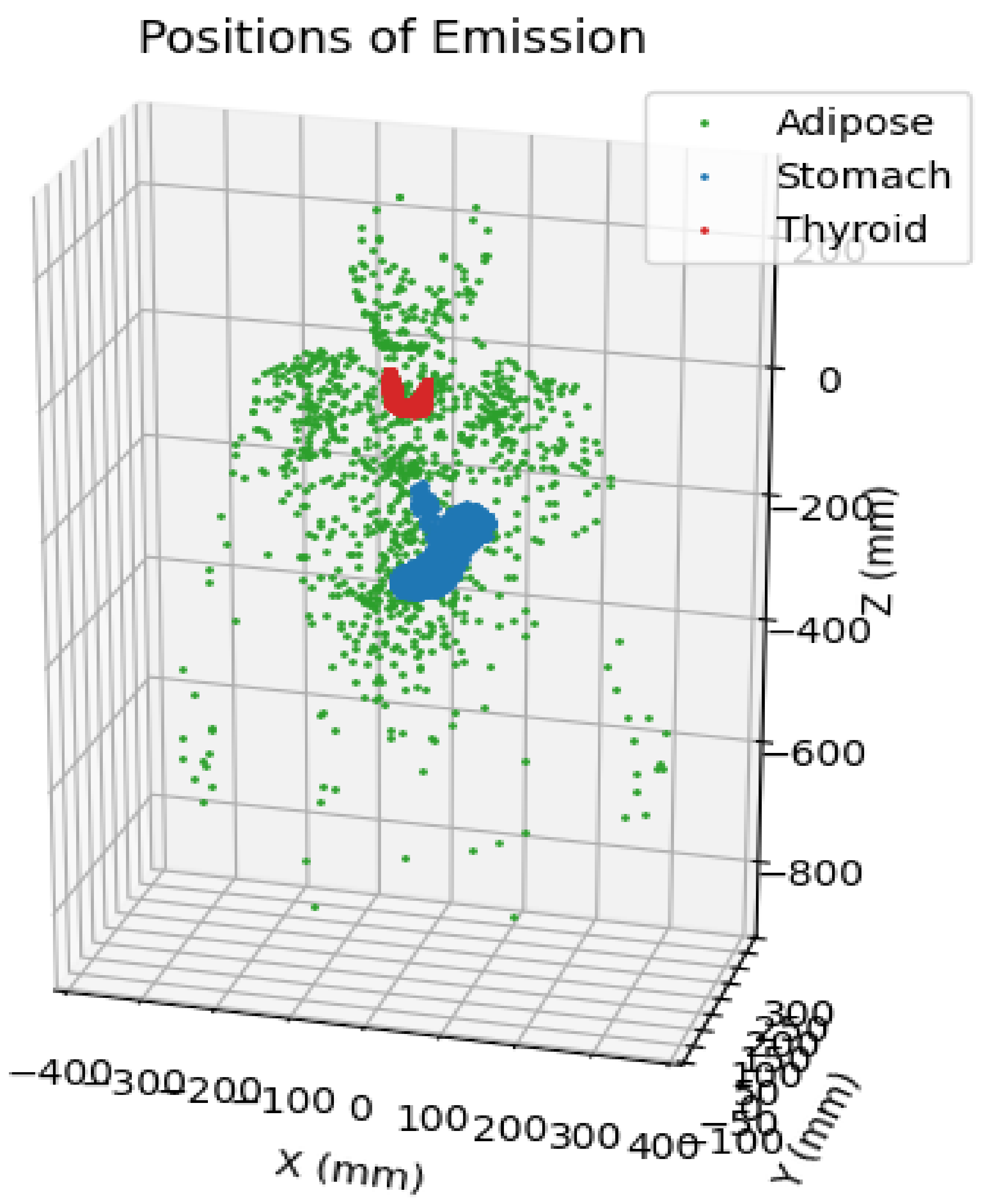

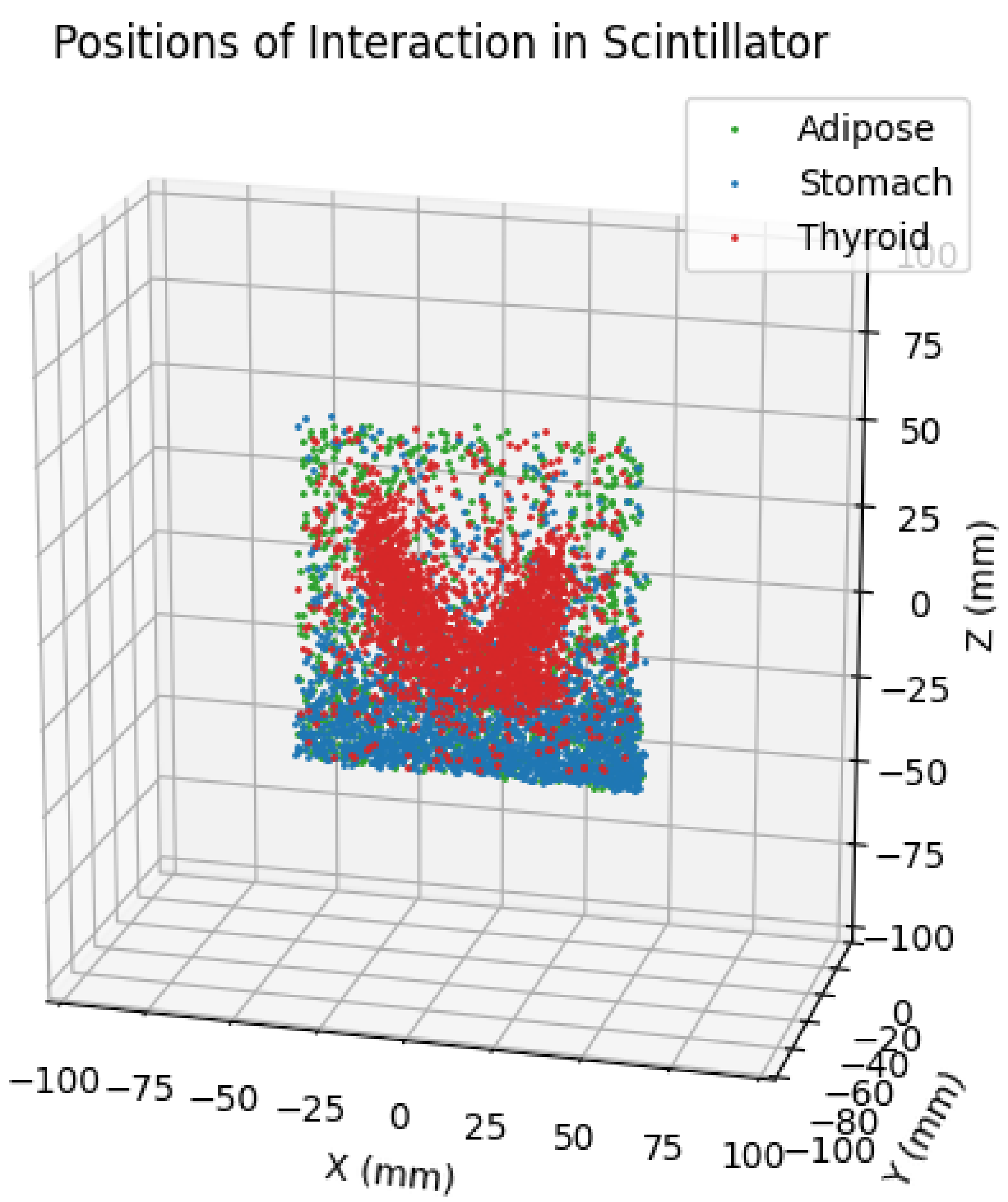

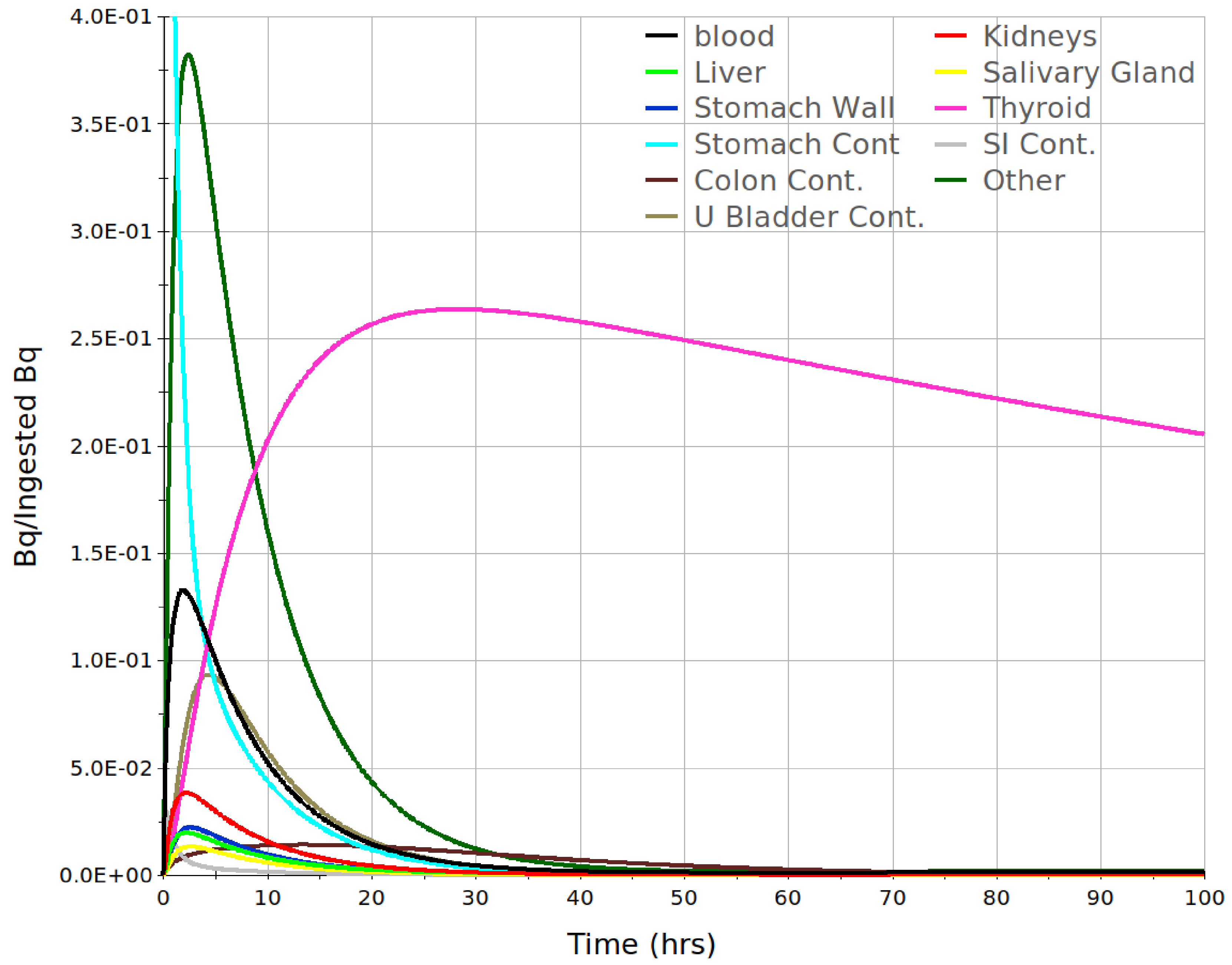

[1] R. W. Leggett, "A Physiological Systems Model for Iodine for Use in Radiation Protection," *Radiation Research*, vol. 174(4), 2010

The shielding optimization

15% uptake in the thyroid

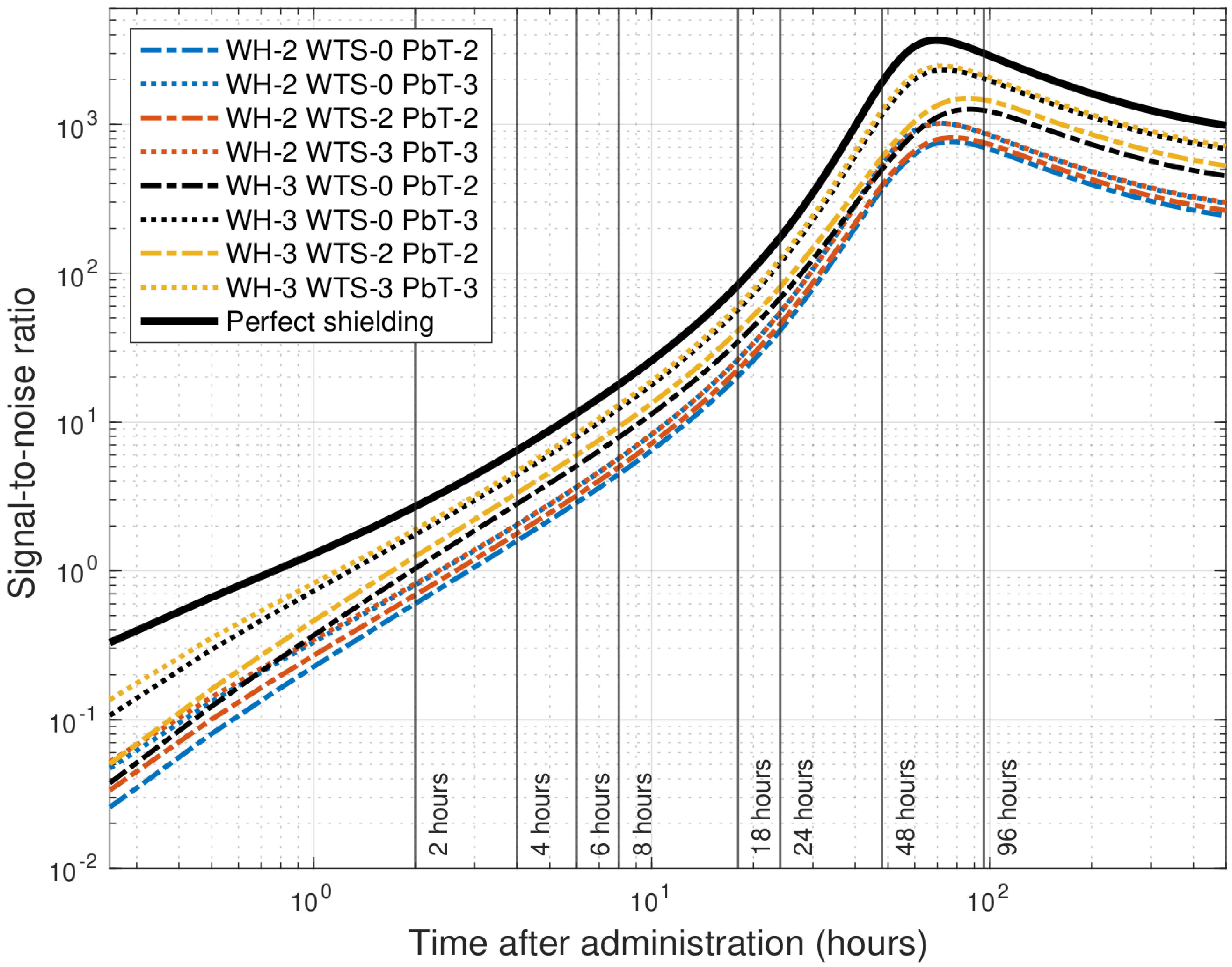

Best shielding (trade-off between SNR and size/ weight of the mobile camera)

- Front of the camera : 3 cm Tungsten
- Back & sides of the camera : 3 cm Lead

SNR at 6 hours after administration :

- Perfect shielding : 11.5
- Chosen configuration : 8
- Lowest shielding : 1.3

Overall mecanical dimensions

Towards a fully operational clinical mobile gamma camera dedicated to thyroid imaging

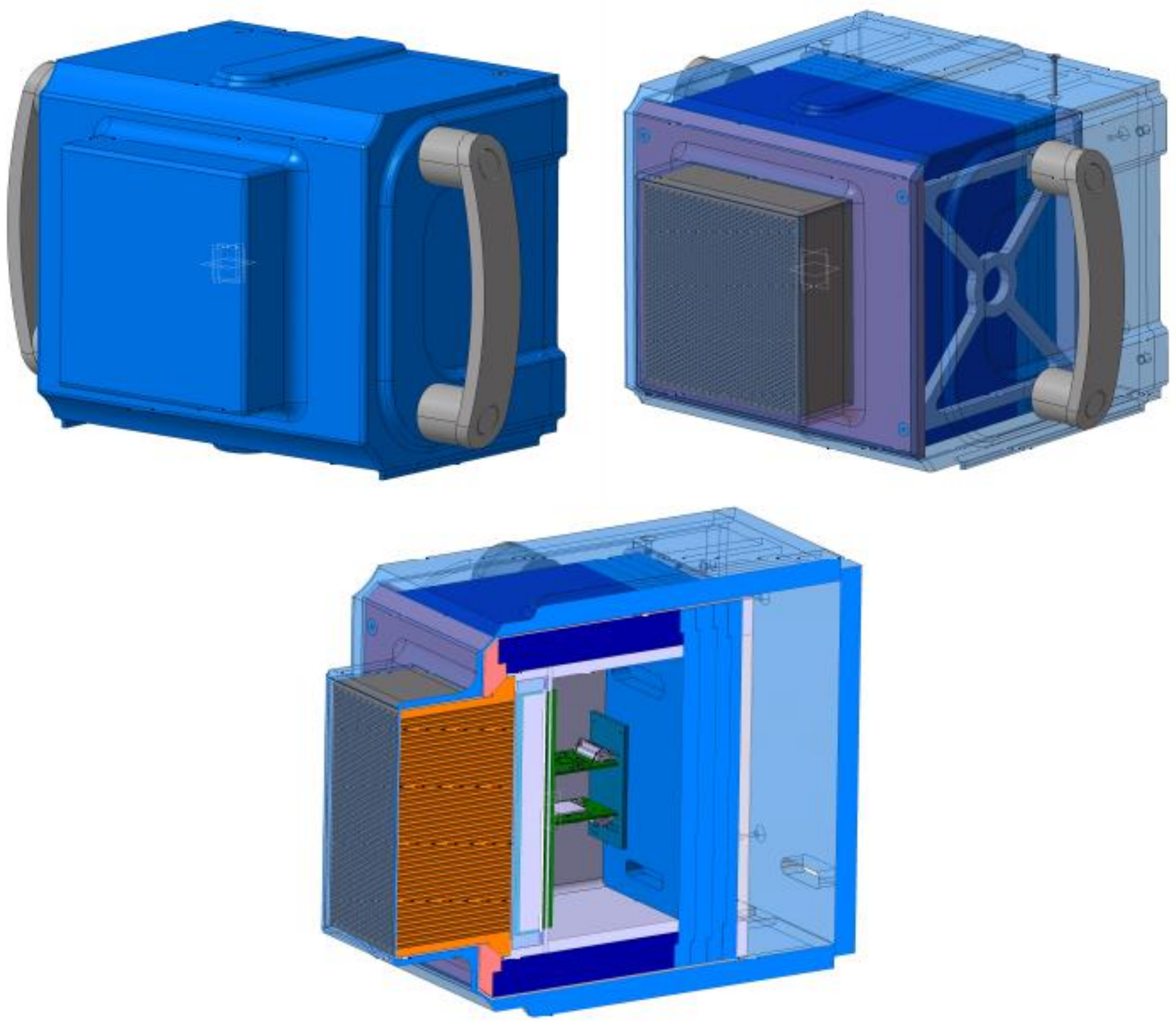

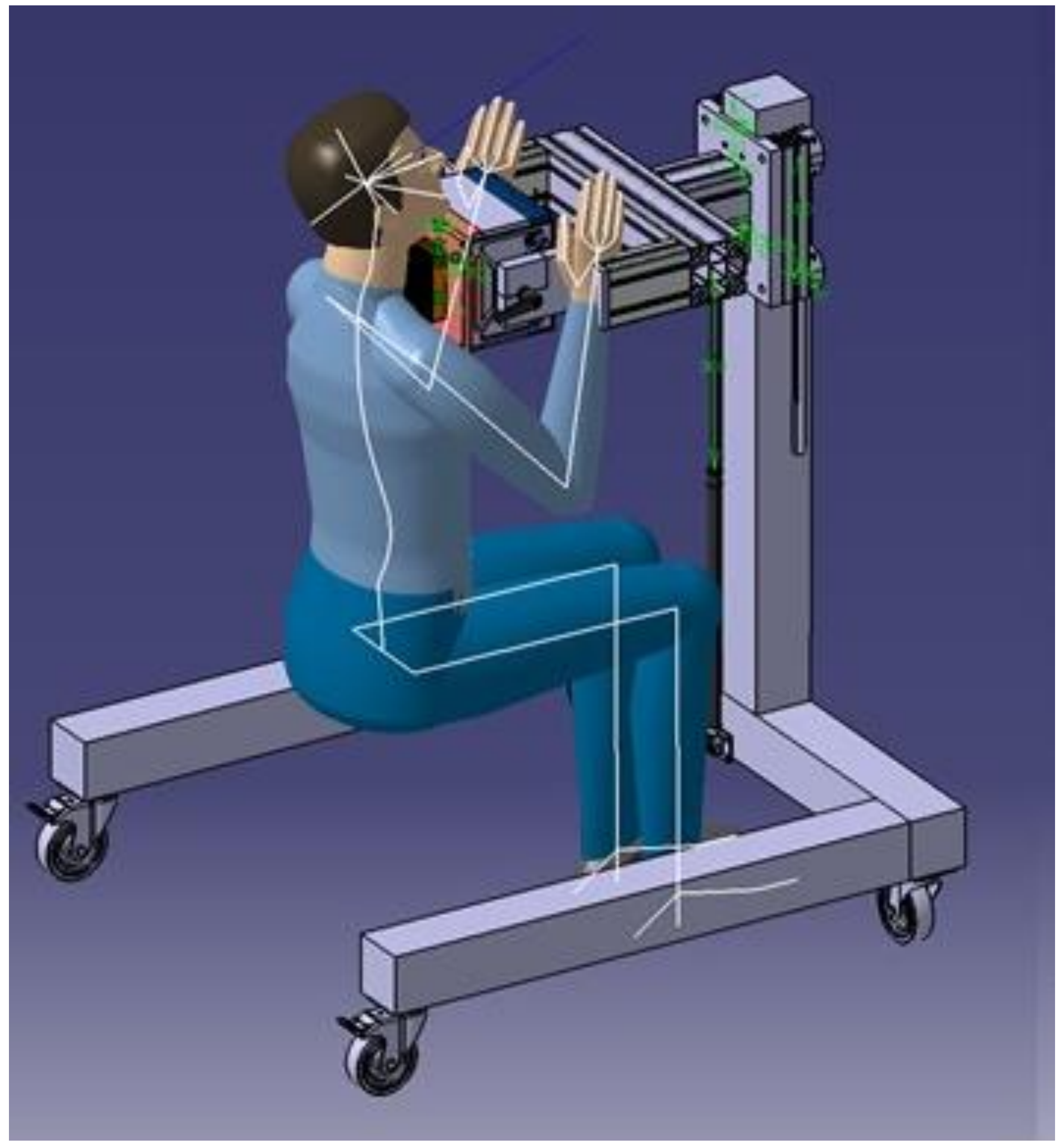

- Overall dimensions : 18x18x20 cm^3
- Total weight : 50 kg (including 30 kg lead shielding)
- Collimator weight : 9 kg

Summary and Conclusion

A 10x10cm^2 field of view clinical prototype is currently under development, dedicated to the patient specific dosimetry in radioiodine treatment of thyroid diseases

✓ Energy resolution <8% FWHM will reduce the influence of scattered events on image contrast and sensitivity

✓ Intrinsic spatial resolution ≤ 1 mm FWHM will reduce partial volume effect and leads to better ROI estimation

✓ Two image reconstruction algorithms: fast Neural Network for Online monitoring and accurate fitting method for Offline reconstruction

✓ Counting rate ~50 kcps. Next upgrade up to 300 kcps by implementing an optical fiber transmission line

Next steps

- ✓ **Calibration of the camera and evaluation of the accuracy and robustness of the quantification protocol** (correction methods, integration of different angular views, ...) using 3D phantoms
- ✓ **Clinical feasibility** study for the radioiodine treatment of differentiated thyroid cancers and benign thyroid diseases : interest to better correlate the dose delivered to the expected dose, as well as to the observed clinical effects (destruction of tumor remnants, thyroid function, toxicity on salivary glands).
- ✓ Determine the best methodological way to integrate available data (mobile camera, SPECT, counting probe…) in order **to reduce uncertainties of the absorbed dose evaluation. Implementation of innovative propagation methods based on Bayesian networks to estimate dose-related uncertainties.**

Acknowledgments

IRSN
INSTITUT DE RADIOPROTECTION ET DE SÛRETÉ NUCLÉAIRE

Tiffany Beaumont
David Broggio
Mohamed Bensiali
Estelle Davesnes
Aurélie Desbrée

IJCLab Irène Joliot-Curie

Carlotta Trigila
Yves Charon
Françoise Bouvet
Laurent Ménard
Laurent Pinot
Marc-Antoine Verdier

Denis Reynet
Harald Ramarijaona
Aurelien Blot

INSTITUT UNIVERSITAIRE DU CANCER DE TOULOUSE Oncopole
INSTITUT CLAUDIUS REGAUD

Olivier Caselles
Laviana Vija
Delphine Vallot

Mathieu Sinigaglia
Slimane Zerdoud

Hôpitaux universitaires Paris-Sud
Antoine-Béclère Bicêtre Paul-Brousse

Luis Ammour
Jad Farah
Aurélie Forbes

With financial support from ITMO Cancer AVIESAN within the framework of the Cancer Plan (AAP Physicancer 2019-2023, THIDOS project)